HHS Public Access

Author manuscript

Inflamm Res. Author manuscript; available in PMC 2020 February 06.

Published in final edited form as:

Inflamm Res. 2018 June ; 67(6): 515–530. doi:10.1007/s00011-018-1141-z.

The nitrone spin trap 5,5-dimethyl-1-pyrroline *N*-oxide dampens lipopolysaccharide-induced transcriptomic changes in macrophages

MD Muñoz[1,2], **MC Della Vedova**[1,2], **PR Bushel**[3], **D Ganini Da Silva**[4], **RP Mason**[4], **Z Zhai**[5], **SE Gomez-Mejiba**[2], **DC Ramirez**[1,*]

[1]Laboratory of Experimental and Translational Medicine, IMIBIO-SL-School of Chemistry, Biochemistry and Pharmacy, National University of San Luis-CONICET, San Luis, 5700 San Luis.

[2]Laboratory of Experimental Therapeutics, School of Health Sciences-IMIBIO-SL, CONICET-National University of San Luis. San Luis, 5700 San Luis, Argentina.

[3]Biostatistics and Computational Biology Branch, NIEHS, NIH, USDHHS, RTP, 27709 NC, USA

[4]Immunity, Inflammation and Disease Laboratory, NIEHS, NIH, USDHHS, RTP, 27709 NC, USA.

[5]Department of Dermatology, University of Colorado Denver, Aurora, 80045 CO, USA

Abstract

M1-like inflammatory phenotype of macrophages plays a critical role in tissue damage in chronic inflammatory diseases. Previously, we found that the nitrone spin trap 5,5-dimethyl-1-pirroline *N*-oxide (DMPO) dampens lipopolysaccharide (LPS)-triggered inflammatory priming of RAW264.7 cells. Herein, we tested whether DMPO by itself can induce changes in macrophage transcriptome, and that these effects may prevent LPS-induced activation of macrophages. To test our hypothesis, we performed a transcriptomic and bioinformatics analysis in RAW264.7 cells incubated with or without LPS, in the presence or in the absence of DMPO. Functional data analysis showed 79 differentially expressed genes (DEGs) when comparing DMPO vs Control. We used DAVID databases for identifying enriched gene ontology terms and Ingenuity Pathway Analysis for functional analysis. Our data showed that DMPO vs Control comparison DEGs are related to downregulation immune-system processes among others. Functional analysis indicated that interferon-response factor 7 and *toll*-like receptor were related (predicted inhibitions) to the observed transcriptomic effects of DMPO. Functional data analyses of the DMPO+LPS vs LPS DEGs were consistent with DMPO dampening LPS-induced inflammatory transcriptomic profile in RAW 264.7. These changes were confirmed using Nanostring technology. Taking together our data, surprisingly, indicates that DMPO by itself affects gene expression related to regulation of immune system and that DMPO dampens LPS-triggered inflammatory transcriptomic profile. Our data provide critical data for further studies on the possible use of DMPO as a structural platform for the design of novel mechanism-based anti-inflammatory drugs.

[*]To Whom Correspondence should be addressed: Dr Dario C Ramirez, Laboratory of Experimental and Translational Medicine, CONICET-UNSL. Phone +5492665030904. ramirezlabimibiosl@ymail.com.

DISCLOUSURE OF ONCLIFCT OF INTEREST

Authors declare no competing conflict of interest

Keywords

macrophage; lipopolysaccharide; inflammation; transcriptomics; DMPO

INTRODUCTION

Inflammation is an essential and protective response of mammalian cells against irritation. However, a chronic inflammatory condition can lead to tissue damage due to an excessive production of reactive biochemical species (RBS) (oxygen, nitrogen, sulphur and halogen-derived reactive species) and inflammatory mediators (cytokines, chemokines and enzymes) [1]. These mediators are mainly produced by innate immune cells, such as macrophages that acquire an inflammatory phenotype at irritated sites. This phenotype of macrophage results from transcriptomic changes towards and inflammatory M1-like profile[2].

The most well-known model of inflammatory activation of macrophage is the priming of RAW264.7 cells induced by bacterial lipopolysaccharide (LPS). In macrophages, Gram negative bacterial LPS is sensed by homo- or hetero-dimeric membrane *toll*-like receptors, particularly TRL-4[3]. Downstream binding of LPS to TLR-4, signaling proceeds throughout a MyD88 dependent pathway that includes the activation of MAPK kinases and a TRIF-mediated signaling pathways that include activation interferon regulatory factors (IRFs) [4]. MyD88 dependent pathway ends in nuclear translocation of the master regulator of the inflammatory response, nuclear factor (NF)-κB and production of proinflammatory cytokines, adhesion molecules and enzymes [5]. TRIF-mediated pathway activation results in type-1 interferon secretion and activation of IRFs[6]. Thus, LPS triggers a number of transcriptional changes in macrophages causing its inflammatory priming. These transcriptomic changes are accompanied by an exaggerated production of RBS, which include radical and non-radical species. Reactive oxygen species (ROS), in particular H_2O_2 have been suggested as secondary messengers in redox signaling and inflammatory activation of macrophages[7].

Antioxidants, such as L-ascorbate, urate or glutathione (GSH) can stop free radical reaction throughout becoming itself a free radical by the radical being scavenged and thus regenerating the native molecule[8, 9]. Unlikely those, spin traps are low-molecular-weight compounds that covalently binds to radical sites in small or large radicalized molecules, and thus can stop free radical-chain reactions that otherwise end in end-oxidation products[10]. Among spin traps, nitrone and nitroxide compounds are the most used in free radical research. Nitrone compounds, such as 5,5-dimethyl-1-pyrroline *N*-oxide (DMPO) and *N*-*tert*-butyl-α-phenylnitrone (PBN) offer particular properties that make them suitable for free radical research in cells and organisms. Particularly, DMPO offers interesting properties including low toxicity, known pharmacokinetics, easy diffusion thorough cell membranes and efficient trapping of free radicals [11–13].

The nitrones PBN and DMPO have been studied for its antioxidant and anti-inflammatory activities, however therapeutic properties of DMPO have been far less studied than those of PBN. As to date PBN derivatives, such as NXY-059 have reached phase III in clinical trials [14, 15]. However, in vivo effects of DMPO are ill defined. Limited data have demonstrated

that pre-administration of DMPO reduces the mortality associated with endotoxin-induced shock in the rat [16], and also it has been shown to protect against reperfusion-induced injury or arrhythmias in isolated rat heart models [17]. Most of these effects have been linked to its free radical-spin trapping properties.

By using DMPO as a tool we have studied the intracellular localization and identity of radicalized protein and DNA in cells, tissues and whole animals [18] [19]. Previously we showed that DMPO reacts with radicalized proteins inside the cell and prevents its further oxidation in a model of LPS-induced priming of murine macrophage-like cell line RAW 264.7[20]. Interestingly DMPO dampened macrophage LPS-driven activation involving nitric oxide (NO) and inflammatory chemokine production by inhibition of NF-κB signaling pathway at early time points after stimulus (15 minutes)[21]. These effects cannot be explained by DMPO scavenging ROS, thus interfering in ROS-dependent signaling, because the rate constant of DMPO reacting with superoxide is slower than the reaction constant of DMPO reacting with radicalized proteins[22, 23]. These evidence suggest that the protective effects afforded by DMPO on macrophages are not only linked to its spin trapping properties.

Herein we used transcriptomic analysis to test whether DMPO causes transcriptional changes that may explain its anti-inflammatory effects on LPS-induced priming of macrophages. This information is critically needed before DMPO or structural analogues proceed to the development of new anti-inflammatory drugs.

MATERIALS AND METHODS

Cell culture

RAW 264.7 cells were obtained from American Type Culture Collection (TIB-71, Rockville, MD) and grown in DMEM-F12 medium supplemented with 10% fetal bovine serum (Natocor, Argentina) at 37 °C in a 5% CO_2 incubator. Cells between passages 4 and 12 were used in this study.

LPS and DMPO treatments

LPS (*Escherichia coli* serotype 055:B5, Cat# L2637) was from Sigma (St. Louis, MO). DMPO was from Dojindo Molecular Technologies (Cat# D-04810, Kumamoto, Japan). Cells were cultivated on 25 or 75 ml T-flasks and allowed to attach for 24 h, then the medium was removed and replaced with the indicated medium with DMPO and/or LPS. DMPO was used at 50 mM in this study. According to our earlier studies, LPS at 1 ng/ml was a non-cytotoxic concentration that primed RAW 264.7 cell to produce significant nitric oxide (NO) [20]. DMPO was mostly used at 50 mM in this study because it could inhibit LPS (1 ng/ml)-induced priming, without significant cytotoxicity as assessed by trypan blue influx, lactic-dehydrogenase release and 3-(4,5-dimethylthiazol-2-yl)-2,5-diphenyltetrazolium bromide (MTT)-reduction assay[20].

NO production assay

Nitrite accumulation in culture medium was measured as an indirect indicator of nitric oxide (•NO) synthesis. 10^5 RAW 264.7 cells were seeded on 96-well microplates and stimulated with different concentration of LPS in the presence or in the absence of 50 mM DMPO for 24 h (final volume 200 μl). After incubation culture medium was collected for nitrite measurement using the Griess reaction. Sodium nitrite was used to produce the standard curve.

RNA isolation for microarray and nCounter experiments

RAW 264.7 cells were incubated in T-75 flask by triplicate with or without 1 ng/ml LPS in the presence or in the absence of 50 mM DMPO. Cells incubated with DMEM culture medium were used as control. After 6 h incubation, cells were washed with PBS, scrapped and pelleted down at 1000*g* for 5 min. centrifugation. Resulting pellet was used for RNA extraction using RNAeasy MIDI kit (QUIAGEN). Purified RNA was quantified using NanoDrop® and quality was assessed by using the Bioanalizer® (Agilent, Santa Clara, CA). 50 μg of RNA was then hybridized with a Mouse genome Set microarray chip (Illumina, ver. 6.1–38000 transcripts) and a Mouse Immunology Codeset (Nanostrings, NS_Immunology_C2269–547 transcripts) as indicated by manufacturer instructions.

Microarray experiment data treatment

Raw pixel intensity data acquired from scanning of the microarrays was background subtracted, log2 transformed and quantile normalized. Probes were filtered if they did not meet the 0.05 quantile (5^{th} percentile) threshold in at least 9 of 12 arrays and then imputed with 6.75111 (the value at the 5^{th} percentile). The filtering removed 1117 probes leaving a total of 37555 remaining probes. A one-way analysis of variance (ANOVA) was used to model the data and then to determine differentially expressed genes (DEGs), the following contrasts were performed: DMPO versus Ctrl; LPS versus Ctrl; DMPO+LPS versus LPS. DEGs lists obtained using a false discovery rate (FDR[24]) < 0.05 and absolute fold change > 1.5 criteria were represented in a Venn diagram using Bioinformatics and Evolutionary Genomics web tool (http://bioinformatics.psb.ugent.be/webtools/Venn/) and in pie chart using Microsoft Excel 2007.

Functional Analysis of DEGs lists

Generated DEG list were analyzed using the Functional Annotation tool of DAVID (Database for Annotation, Visualization and Integrated Discovery, Bioinformatics Resources 6.8, NIAID/NIH), Top KEGG pathways and Gene Ontology (GO) terms were listed. DEGs lists were also analyzed using Functional Analysis tool of Ingenuity Pathway Analysis (IPA) Software (QUIAGEN). Summary, Associated Canonical Pathways, Top upstream regulators and Associated Networks from IPA results were used for this publication.

mRNA detection and analysis with nCounter

Gene expression was examined using the NanoString© platform (www.nanostring.com) utilizing Nanostrings Mouse Immunology Codeset (NS_Immunology_C2269) consisting of 547 endogenous and 14 housekeeping genes. 50 ng of each total RNA sample was prepared

as per the manufacturer's instructions. Gene expression was quantified on the nCounter Digital Analyzer ™ and raw and normalized counts were generated with nSolver (v3.0) ™ software. Data were normalized utilizing the manufacturer's positive and negative experimental control probes, as well as the housekeeping gene GAPDH. Results are expressed as mean value ± SEM. Effects were assessed using the Student's *t* test. A difference between treatment groups with $P<0.05$ was considered statistically significant.

Preparation of cell lysates

Following treatments with LPS for the indicated times, RAW 264.7 cell activation was stopped by the removal of medium and addition of ice-cold PBS [25]. In brief, whole cell lysates were prepared and used to detect proteins of interest. Cells were lysed with the CelLytic M lysis solution (Sigma) containing 1% (v/v) protease inhibitor cocktail (Amresco). Cell debris was removed by centrifugation at 12,000 g for 15 min at 4 °C, and the resultant supernatants were stored at −80 °C until use. The protein concentrations in cell lysates were determined using a BCA protein assay kit (Pierce Labs, Rockford, IL) with bovine serum albumin as standard.

Western blot

Cell lysates were mixed with 4 × SDS NuPAGE sample loading buffer (Invitrogen). After heat denaturation, equal amounts of cellular proteins were separated on 4–12% reducing NuPAGE Bis-Tris Gels (Invitrogen), followed by electrotransfer onto a nitrocellulose membrane (0.2 μM pore size). After blocking with 5% non-fat milk in PBS, the immunoblot was performed by incubation with a primary antibody overnight at 4 °C, and then fluorescence goat anti-rabbit or goat anti-mouse IgG secondary antibody for 1 h at room temperature. The immunocomplexes were visualized usingFluorChem HD2 imager (Alpha Innotech Corp., San Leandro, CA). The following primary antibodie was used from ABCAM: IRF7- Catalog Number: Ab-109255. Gliceraldehide-phosphate deshydrogenase (GAPDH) from ABCAM was used as loading control. Image was analyzed using free software ImageJ®.

IFN-β determination

To measure the production of IFN-β cytokine, RAW 264.7 cells were grown 25 ml flasks and treated with LPS and/or DMPO for 24 h. The culture medium was collected and assessed using commercial Mouse IFN-β ELISA kit (N° MIFNB0; R&D Systems; MN; USA).

Statistical analysis

Results are expressed as mean value± s.e.m. Effects were assessed using the Student's t test. A difference between treatment groups with $P<0.05$ was considered statistically significant.

RESULTS

Effects of DMPO, LPS and DMPO+LPS on RAW 264,7 cells transcriptome

We previously showed that DMPO decreases LPS-triggered M1-linked pro-inflammatory cytokine (IL-1β, IL-6 and TNF-α) and NO production in RAW 264,6 cells[21]. Herein we were able to reproduce those data by showing that incubation of RAW264.7 cells for 24 h with a low concentration of LPS such as 1 ng/ml was enough to cause significant nitrite accumulation in the culture medium (Fig 1A). Furthermore, we show that addition of 50 mM DMPO to the culture medium dampens this LPS-induced nitrite accumulation (Fig. 1B).

Our previous data showed that the reduction of nitrite accumulation in LPS-primed cells caused by DMPO, was consistent with low inducible nitric oxide synthase (iNOS) gene expression and reduction of MAPK signaling[21], but the precise mechanism by which DMPO exerts its transcriptomic effects remains unknown.

To achieve a deeper understanding of how DMPO causes its anti-inflammatory effects herein we studied its transcriptional effects on resting macrophages in the presence or in the absence of DMPO using microarray technology. We also used RAW 264,7 cells treated for 6 h with or without 50 mM DMPO, in the presence or absence of 1 ng/ml LPS, to understand how DMPO modulates the transcriptional changes induced by LPS. After treatment we isolated mRNA and analyzed the transcriptome using an Illumina® Mouse Genome chip. Data was obtained (Fig. 2), background subtracted, normalized and statically treated using ONE-WAY ANOVA (FDR= 0.05) to generate lists of DEGs.

We graphed the lists of differentially expressed genes in a Venn diagram using Bioinformatics and Evolutionary Genomics web tool and the results showed 18 genes that were present in all three comparisons (Fig. 3A). The treatment of RAW 264,7 cells with 50 mM DMPO for 6 hours in absence of LPS resulted in 79 genes differentially expressed. 23 genes were up regulated whereas 56 were downregulated (Fig. 3B). The effect of LPS was analyzed as positive control for inflammatory activation and the data showed 949 genes differentially expressed respect to untreated cells, 543 were up-regulated and 406 were downregulated (Fig. 3B). Treatment with DMPO in the presence of LPS was also tested and gene expression was compared to the LPS condition. The analysis showed 215 genes, 54 upregulated and 161 downregulated in respect to LPS treated cells (Fig. 3B).

These results indicate that LPS treatment generates major changes in macrophage transcriptome with most genes upregulated (57%). Compared to LPS effect, DMPO by itself generates fewer changes in the transcriptome and these changes are predominately linked to downregulated gene expression (71%). When comparing DMPO+LPS vs LPS, 75% of genes were downregulated indicating that DMPO is clearly dampening the effects caused by LPS.

Functional Analysis of DMPO effects on the transcriptome of RAW 264.7 cells in the absence of LPS (DMPO vs Control DEGs)

In order to establish a relationship between the list of genes affected by DMPO and biological functions we used DAVID database for identifying enriched GO terms. Functional Annotation clustering showed that DMPO treatment affects those genes associated with

response to viruses, immune system processes and negative regulation of *Toll*-like receptor signaling pathways among others (Table 1).

In order to identifying enriched biological pathways and upstream regulators that may be regulated by DMPO we submitted the same gene list to IPA software. IPA results are summarized in Figure 4 were cardiac β-adrenergic signaling, nitric oxide and interferon signaling are among the top associated canonical pathways (Supplementary Fig. 1).

This analysis also predicted that transcription factors related to interferon (IRF7 and IRF3) and *Toll*-like receptors (TLR 3, 4 and 9) as upstream regulators (Table 2). Their interactions with other related molecules are shown in Figure 5. Top associated network is shown in Supplementary Figure 2.

Taking together, functional annotation clustering with DAVID database and functional analysis using IPA software surprisingly indicate that the effects of DMPO by itself are related to downregulation of immune process, in particular interferon signaling and *Toll*-like receptors.

Functional analysis of LPS on the transcriptome of RAW 264,7 cells as a positive control for macrophage inflammatory activation

In order to identify the genes associated with LPS-related inflammatory activation of macrophages we performed functional analysis on the DEGs in the comparison LPS vs Control cells. We used DAVID database and IPA software for identifying enriched GO terms, canonical pathways and upstream regulators. Results of functional annotation are shown in Table 3 were top enriched GO terms are displayed. KEGG pathways are displayed in Supplementary Table 1.

LPS vs Control DEGs are associated among others with inflammatory response, LPS-mediated signaling pathway (GO terms), TNF-signaling and *Toll*-like receptor signaling pathway (KEGG pathways). IPA results are displayed in Figure 6 and Supplementary Figure 3 (Top-canonical pathways) and 4 (Top-associated network). Upstream regulators are listed in Supplementary Table 2 and their interactions are showed in Figure 7.

Taking together our data obtained using DAVID database and IPA software show unbiased results on LPS vs Control DEGs consistent with previously published results[26].

Functional analysis of DMPO effects on the transcriptome of RAW 264.7 cells in the presence of LPS (DMPO+LPS vs LPS DEGs)

In order to understand the effects of DMPO on the transcriptome of LPS-primed macrophages we submitted DMPO+LPS vs LPS DEGs to functional analysis using DAVID database and IPA software. Functional annotation clustering results are listed in Table 4 (GO terms) and Table 5 (KEGG pathways).

These results indicate that the genes affected by DMPO in LPS-primed RAW 264.7 cells were related to cellular response to LPS, response to viruses and cellular response to IFN-β among others GO terms. These genes were also associated with TNF-α signaling pathway,

Toll-like receptor and MAPK signaling pathway, among others KEGG pathways (Table 5). These data are consistent with DMPO affecting several signaling pathways triggered by LPS[26]. Moreover, IPA analysis showed TLR receptors (3, 4 and 9) as predicted upstream regulators (Fig. 8 and Table 6) and canonical pathways related to communication between immune cells as enriched (Supplementary Fig. 5). Top associated network is displayed in Supplementary Figure 6.

It is important to highlight that most of the upstream regulators are predicted as inhibitions (Table 6), which is consistent with DMPO dampening the entire signaling related to TLRs triggered activation by LPS. Figure 9 displays how the molecules predicted are related to each other and also shows the behavior of genes downstream of these interactions. CCL2, CCL7, IRF7 and CD40 are highlighted in green indicating down regulation of its mRNAs expression in the DMPO+LPS vs LPS comparison.

All together comparison analysis of DMPO+LPS vs LPS DEGS indicates that DMPO dampens LPS signaling in different molecular pathways (MyD88-dependent and TRIF-dependent).

Confirmation of MyD88-dependent pathway inhibition by DMPO in LPS stimulated RAW 264.7 cells.

In order to confirm the results obtained by microarray technology, the same experiment was used for gene expression analysis using nCounter® technology. Over 500 transcripts were analyzed, Figure 10 displays the gene expression of molecules highlighted in IPA analysis and DAVID functional clustering: CCL2, CCL7 proteins as well as cytokines such as IL-6 and TNF-α.

Ncounter® results are consistent with previously published data were Myd88-dependent signaling pathway related proteins such as Inducible nitric oxide synthase (iNOS) and ciclooxygenase-2 (COX-2) were measured at protein levels and functional activity together with IL-6 and TNF-α production by ELISA [21, 27]. Moreover Figure 10 results confirm the behavior of genes highlighted by functional analysis of DMPO+LPS vs LPS DEGs list related to MyD88-dependent pathway such as CCL2, CCL7, IL-6 and TNF-α.

Confirmation of TRIF-dependent pathway inhibition by DMPO in LPS stimulated RAW 264.7 cells.

In order to confirm data obtained by microarray technology related to TRIF-dependent signaling pathway inhibition we determine the expression IRF7 and IFN-β mRNA using nCounter® technology. Moreover we measure IRF7 protein levels by western-blot and its activity by measuring IFN-β by ELISA technique. Results are shown in Figure 11.

Results displayed in Figure 11 indicate that the addition of DMPO has no effect on the IRF7 mRNA levels after 6 hours of incubation (Fig. 11 A). However DMPO was able to reduce the expression of IRF7 protein levels and IFN- β after 24 hours of incubation (Fig. 11 B; C and D).

Taking together these results are consistent with data obtained using microarray technology and functional analyses were LPS-triggered TRIF-dependent signaling was blocked when DMPO is added to culture medium.

DISCUSSION

Herein we provide unbiased evidence about the transcriptomic effects of DMPO in RAW 264.7 macrophage-like cell line. We also show that DMPO dampens most of the transcriptomic changes caused by LPS in these cells. These evidences provide unbiased data about the mechanism-based effects of DMPO and possibly other nitrones with anti-inflammatory effects.

Nitrone spin traps such as PBN and DMPO were originally developed with the purpose of trapping and stabilizing free radicals, thus making possible their study by ERS or immuno-spin trapping[12, 13]. However, they have shown other properties that made them interesting for pharmacological application as anti-inflammatory drugs, in particular for modifying the phenotype of macrophages toward a M2-like anti-inflammatory phenotype. As today DMPO or any of its structural analogs have not been moved into the drug development pipeline. On the other hand, PBN-derived compounds have been probed in different models and have reached phase III clinical trials but mechanisms of its effects remain obscure[13]. This situation could be due to DMPO synthesis being really expensive in comparison to PBN and related compounds, and also because transcriptomic effects of DMPO on inflammatory cells remain ill defined. The production of mechanism based–drugs is an emerging field that will lead to safer drugs, especially anti-inflammatory drugs.

PBN and DMPO have been probed to have anti-inflammatory properties on several experimental models. Both spin traps are able to dampen LPS-triggered signaling related to MAPK, Akt, iNOS, COX-2 and pro-inflammatory cytokines [21, 28] suggesting that these effects may be related its nitrone motifs. Moreover, these anti-inflammatory effects cannot be explained by the superoxide radical anion scavenging properties of the spin trap due to a low reaction rate constant in both cases[22]. It has been suggested that DMPO reacts with protein and DNA-centered radicals thus interfering the chain reaction for radical production and redox-dependent signaling process [18, 20]. In vivo, DMPO competes with natural anti-oxidant molecules (such as glutathione and L-ascorbate) for free radicals and radicalized macromolecules, thus high doses of the spin trap are needed to overcome the competing reactions[29]. These competing reactions have in most cases rate constants much larger than that of DMPO with macromolecule-centered radicals, thus formation of nitrone adducts is a kinetically unfeasible process. Currently the exact mechanism by which spin traps exert their anti-inflammatory effect remains unknown.

With the purpose of achieving a better understanding on how DMPO affects macrophage's biology we aimed at studying the transcriptome in a wider approach using microarray technology. Firstly, we analyzed the effect of 50 mM DMPO incubation for 6 h on RAW 264.7 cells in the absence of LPS. DMPO was able to affect the expression levels of 80 genes (compared to control) with 71% of them being downregulated. Interestingly, functional analysis of these genes using functional annotation clustering (DAVID database)

and IPA software indicates that DMPO affects the expression of genes related to negative regulation of immune system processes and inflammatory responses with IRF7 predicted as the top upstream regulator. DMPO was also able to upregulate genes encoding enzymes critically involved in GSH biosynthesis (Supplementary Fig. 1). These changes on the transcriptome cannot be explained by DMPO reacting with protein centered radicals that are necessary for redox-dependent signaling in resting cells, because the affected genes are almost exclusively related to immune system processes. If DMPO would interfere with redox-dependent signaling, several others biological functions would be compromised, due to the promiscuity of free radical reactions.

Secondly, we analyzed the effects of the spin trap on the transcriptome of LPS-primed cells. When DMPO was added simultaneously with LPS on RAW 264.7 cells for 6 h the overall gene expression changed in 215 genes of which 75% were downregulated when compared to LPS stimulated cells. This transcriptomic profile indicates that DMPO is clearly dampening those transcriptomic effects triggered by LPS. Furthermore, we performed functional analysis on these genes using DAVID database and IPA software and the results are consistent with DMPO interfering with both Myd88-dependent and TRIF-dependent pathways of TLR4 activated by LPS (together with other TLRs) and transcription factors related to interferon predicted as inhibited upstream regulators. These effects observed in both activation pathways of TLR-4 were consistent with nCounter® experiments and with previously published data by our group on MyD88-dependent signaling blockage by DMPO in LPS stimulated RAW 264.7 cells [21]. Moreover we also confirmed the effects of DMPO on the TRIF-dependent signaling pathway triggered by LPS in macrophages at protein and activity levels (IRF7 and IFNβ).

Taking together the transcriptomic changes obtained in the presence or in the absence of LPS we can conclude that the effects of DMPO are related to a negative regulation of immune system process, particularly TLRs and IRF signaling. Further studies to define specific sites where DMPO causes these transcriptomic effects are undergoing in order to provide a most robust mechanism of action for this old compound with novel therapeutic properties.

Supplementary Material

Refer to Web version on PubMed Central for supplementary material.

ACKNOWLEDGEMENTS

Authors want to express their gratitude to Dr Bart Frank (OMRF) for early processing of raw microarray data used in this study and to Dr Paula Di Sciullo for excellent technical assistance. This study was supported in part by the following agencies: PICT-3369 (FONCyT, AGENCIA, Argentina), PIP 916 (CONICET) and PROICO 2332 and PROICO 100414 (National University of San Luis). In addition, this research was supported in part by the National Institute of Environmental Health Sciences.

REFERENCES

[1]. Liu YC, Zou XB, Chai YF, Yao YM, Macrophage polarization in inflammatory diseases, International journal of biological sciences 10(5) (2014) 520–9. [PubMed: 24910531]

[2]. Mosser DM, Edwards JP, Exploring the full spectrum of macrophage activation, Nature reviews. Immunology 8(12) (2008) 958–69.

[3]. Jin MS, Lee JO, Structures of the toll-like receptor family and its ligand complexes, Immunity 29(2) (2008) 182–91. [PubMed: 18701082]

[4]. Kawai T, Akira S, The role of pattern-recognition receptors in innate immunity: update on Toll-like receptors, Nature immunology 11(5) (2010) 373–84. [PubMed: 20404851]

[5]. May MJ, Ghosh S, Signal transduction through NF-kappa B, Immunology today 19(2) (1998) 80–8. [PubMed: 9509763]

[6]. Ullah MO, Sweet MJ, Mansell A, Kellie S, Kobe B, TRIF-dependent TLR signaling, its functions in host defense and inflammation, and its potential as a therapeutic target, Journal of leukocyte biology 100(1) (2016) 27–45. [PubMed: 27162325]

[7]. Finkel T, Signal transduction by reactive oxygen species, The Journal of cell biology 194(1) (2011) 7–15. [PubMed: 21746850]

[8]. Halliwell B, Antioxidant characterization. Methodology and mechanism, Biochemical pharmacology 49(10) (1995) 1341–8. [PubMed: 7763275]

[9]. Domazou AS, Koppenol WH, Gebicki JM, Efficient repair of protein radicals by ascorbate, Free radical biology & medicine 46(8) (2009) 1049–57. [PubMed: 19185609]

[10]. Janzen EG, Spin trapping, Methods in enzymology 105 (1984) 188–98. [PubMed: 6328178]

[11]. Janzen EG, Jandrisits LT, Shetty RV, Haire DL, Hilborn JW, Synthesis and purification of 5,5-dimethyl-1-pyrroline-N-oxide for biological applications, Chemico-biological interactions 70(1–2) (1989) 167–72. [PubMed: 2544305]

[12]. Janzen EG, Poyer JL, Schaefer CF, Downs PE, DuBose CM, Biological spin trapping. II. Toxicity of nitrone spin traps: dose-ranging in the rat, Journal of biochemical and biophysical methods 30(4) (1995) 239–47. [PubMed: 8621883]

[13]. Janzen EG, West MS, Kotake Y, DuBose CM, Biological spin trapping methodology. III. Octanol-water partition coefficients of spin-trapping compounds, Journal of biochemical and biophysical methods 32(3) (1996) 183–90. [PubMed: 8844325]

[14]. Lees KR, Zivin JA, Ashwood T, Davalos A, Davis SM, Diener HC, Grotta J, Lyden P, Shuaib A, Hardemark HG, Wasiewski WW, NXY-059 for acute ischemic stroke, The New England journal of medicine 354(6) (2006) 588–600. [PubMed: 16467546]

[15]. Floyd RA, Kopke RD, Choi CH, Foster SB, Doblas S, Towner RA, Nitrones as therapeutics, Free radical biology & medicine 45(10) (2008) 1361–74. [PubMed: 18793715]

[16]. Hamburger SA, McCay PB, Endotoxin-induced mortality in rats is reduced by nitrones, Circulatory shock 29(4) (1989) 329–34. [PubMed: 2688966]

[17]. Zuo L, Chen YR, Reyes LA, Lee HL, Chen CL, Villamena FA, Zweier JL, The radical trap 5,5-dimethyl-1-pyrroline N-oxide exerts dose-dependent protection against myocardial ischemia-reperfusion injury through preservation of mitochondrial electron transport, The Journal of pharmacology and experimental therapeutics 329(2) (2009) 515–23. [PubMed: 19201989]

[18]. Ramirez DC, Mejiba SE, Mason RP, Immuno-spin trapping of DNA radicals, Nature methods 3(2) (2006) 123–7. [PubMed: 16432522]

[19]. Gomez-Mejiba SE, Zhai Z, Akram H, Deterding LJ, Hensley K, Smith N, Towner RA, Tomer KB, Mason RP, Ramirez DC, Immuno-spin trapping of protein and DNA radicals: “tagging” free radicals to locate and understand the redox process, Free radical biology & medicine 46(7) (2009) 853–65. [PubMed: 19159679]

[20]. Zhai Z, Gomez-Mejiba SE, Gimenez MS, Deterding LJ, Tomer KB, Mason RP, Ashby MT, Ramirez DC, Free radical-operated proteotoxic stress in macrophages primed with lipopolysaccharide, Free radical biology & medicine 53(1) (2012) 172–81. [PubMed: 22580125]

[21]. Zhai Z, Gomez-Mejiba SE, Zhu H, Lupu F, Ramirez DC, The spin trap 5,5-dimethyl-1-pyrroline N-oxide inhibits lipopolysaccharide-induced inflammatory response in RAW 264.7 cells, Life sciences 90(11–12) (2012) 432–9. [PubMed: 22285597]

[22]. Finkelstein E, Rosen GM, Rauckman EJ, Paxton J, Spin trapping of superoxide, Molecular pharmacology 16(2) (1979) 676–85. [PubMed: 229403]

[23]. Makino KH, Takuya; Murakami Akira, A mini review: Fundamental aspects of spin trapping with DMPO, International Journal of Radiation Applications & Instrumentation. Part C, Radiation Physics & Chemistry 37(5) (1991) 657–665.

[24]. Hochberg YBY, Controlling the false discovery rate: a practical and powerfull approach to multiple testing, Journal of the Royal Statistical Society. Series B (Methodological) 57(1) (1995) 289–300.

[25]. Gomez-Mejiba SE, Zhai Z, Della-Vedova MC, Munoz MD, Chatterjee S, Towner RA, Hensley K, Floyd RA, Mason RP, Ramirez DC, Immuno-spin trapping from biochemistry to medicine: advances, challenges, and pitfalls. Focus on protein-centered radicals, Biochimica et biophysica acta 1840(2) (2014) 722–9. [PubMed: 23644035]

[26]. Huang H, Park CK, Ryu JY, Chang EJ, Lee Y, Kang SS, Kim HH, Expression profiling of lipopolysaccharide target genes in RAW264.7 cells by oligonucleotide microarray analyses, Archives of pharmacal research 29(10) (2006) 890–7. [PubMed: 17121185]

[27]. Kotake Y, Sang H, Miyajima T, Wallis GL, Inhibition of NF-kappaB, iNOS mRNA, COX2 mRNA, and COX catalytic activity by phenyl-N-tert-butylnitrone (PBN), Biochimica et biophysica acta 1448(1) (1998) 77–84. [PubMed: 9824673]

[28]. Tabatabaie T, Vasquez AM, Moore DR, Floyd RA, Kotake Y, Direct administration of interleukin-1 and interferon-gamma to rat pancreas leads to the in vivo production of nitric oxide and expression of inducible nitric oxide synthase and inducible cyclooxygenase, Pancreas 23(3) (2001) 316–22. [PubMed: 11590329]

[29]. Davies MJ, Hawkins CL, EPR spin trapping of protein radicals, Free radical biology & medicine 36(9) (2004) 1072–86. [PubMed: 15082061]

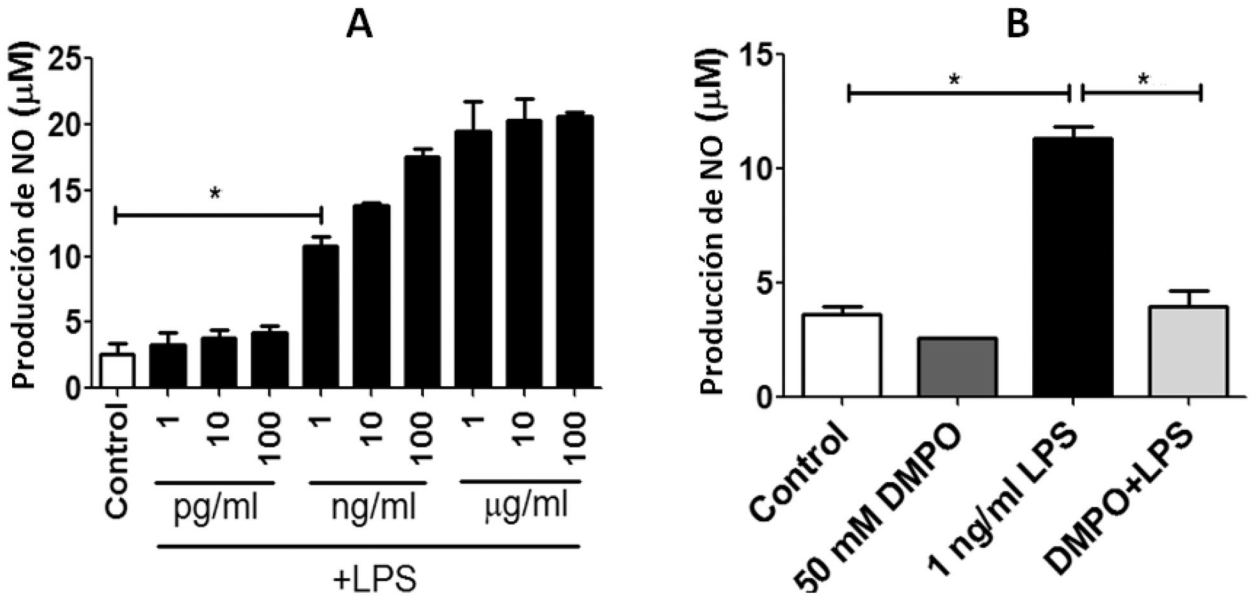

Figure 1: DMPO reduces nitric oxide synthesis in macrophages during priming with LPS.

A) Effects of different concentrations of LPS on NO production in RAW 264.7 cells. 10^5 Cells were treated with increasing amount of LPS. **B)** RAW 264.7 cells were incubated with 1 ng/ml LPS in the presence or in the absence of 50 mM DMPO. After incubation for 24 h nitrite concentration in the medium was determined using the Griess reaction. Results are shown as mean values ± s.e.m. from 3 independent experiments. Data were analyzed using the **t**-test. *P value < 0,001

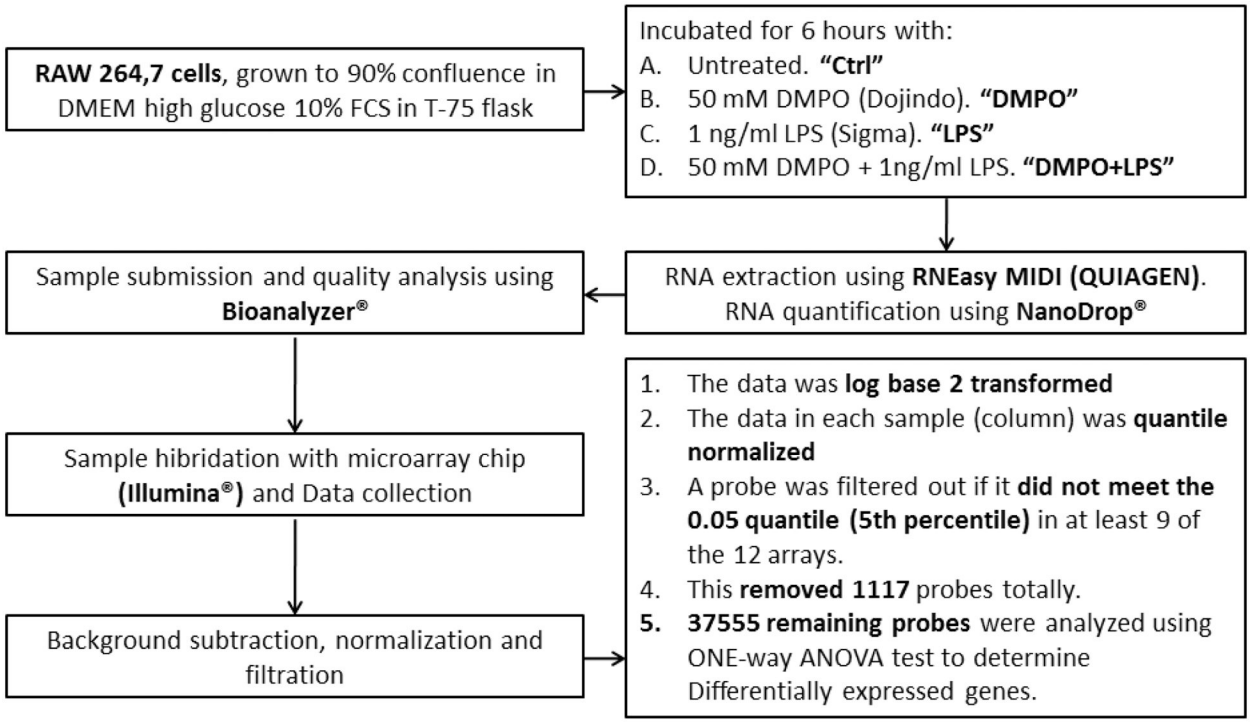

Figure 2: Microarray experiment.

Flux diagram for sample preparation and data collection.

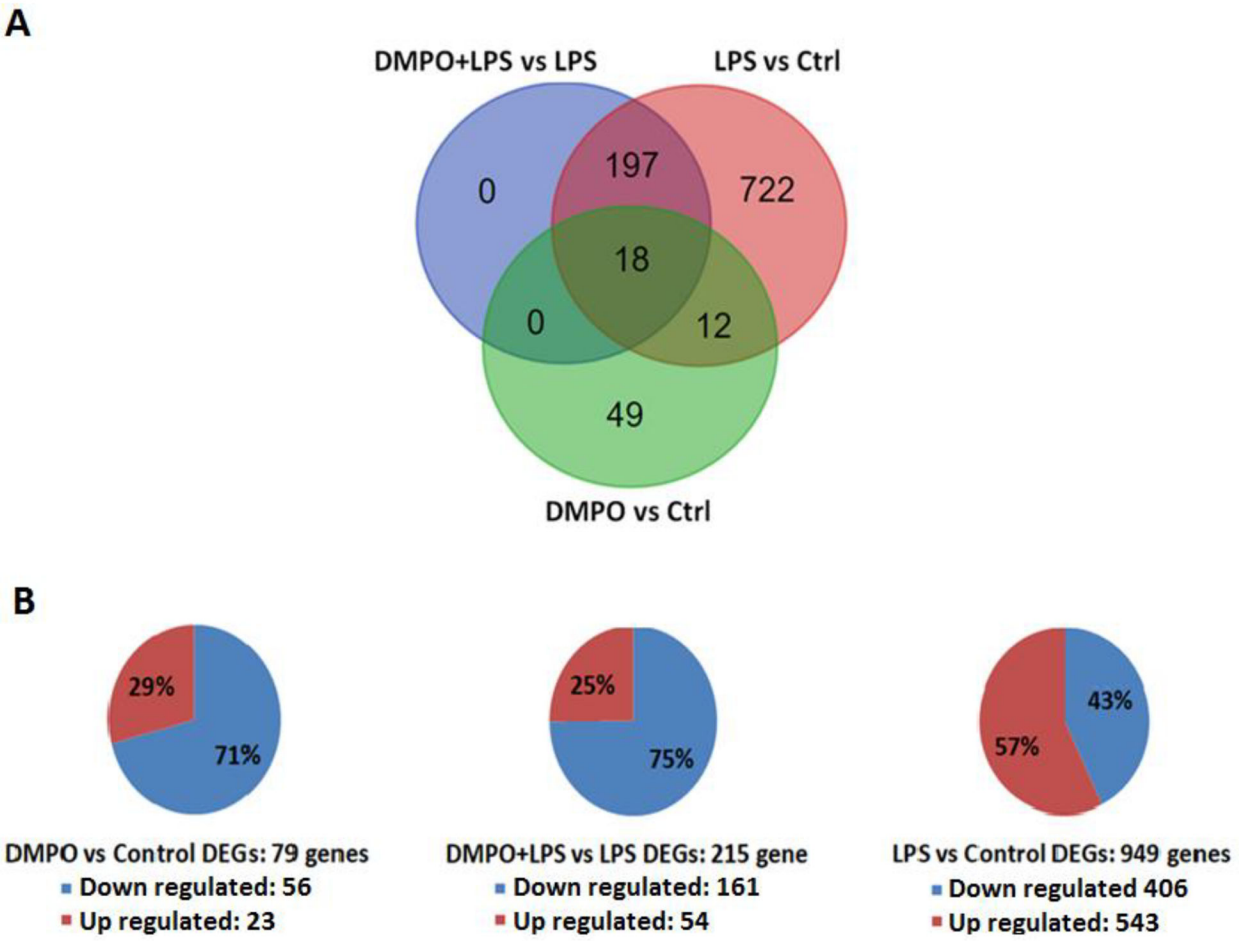

Figure 3: Statistic analysis and data representation: ONE-WAY ANOVA

was performed to determine Differentially Expressed Genes (**DEGs**) for samples compared to control. False Discovery Rate (**FDR**) **Q= 0,05**. Fold change threshold **1,5**. DMPO vs Control: 79 genes; LPS vs Control: 949 genes; DMPO+LPS vs LPS: 215 genes. **A)** Venn diagram for the 3 DEGs lists resulting **B)** Pie charts for DEGs lists behavior respect to control, downregulated genes are shown in blue and upregulated genes are shown in red.

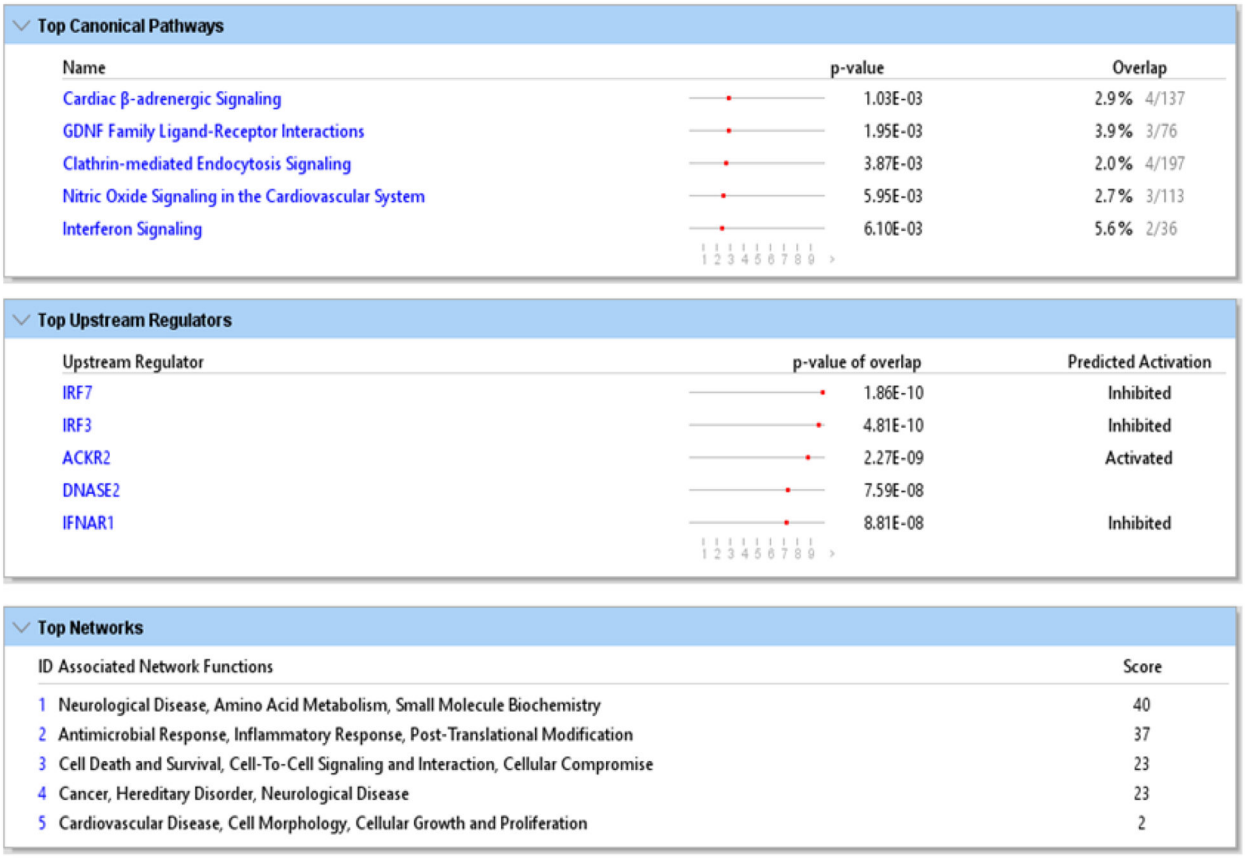

Top Canonical Pathways

Name	p-value	Overlap
Cardiac β-adrenergic Signaling	1.03E-03	2.9% 4/137
GDNF Family Ligand-Receptor Interactions	1.95E-03	3.9% 3/76
Clathrin-mediated Endocytosis Signaling	3.87E-03	2.0% 4/197
Nitric Oxide Signaling in the Cardiovascular System	5.95E-03	2.7% 3/113
Interferon Signaling	6.10E-03	5.6% 2/36

1 2 3 4 5 6 7 8 9 ›

Top Upstream Regulators

Upstream Regulator	p-value of overlap	Predicted Activation
IRF7	1.86E-10	Inhibited
IRF3	4.81E-10	Inhibited
ACKR2	2.27E-09	Activated
DNASE2	7.59E-08	
IFNAR1	8.81E-08	Inhibited

1 2 3 4 5 6 7 8 9 ›

Top Networks

ID	Associated Network Functions	Score
1	Neurological Disease, Amino Acid Metabolism, Small Molecule Biochemistry	40
2	Antimicrobial Response, Inflammatory Response, Post-Translational Modification	37
3	Cell Death and Survival, Cell-To-Cell Signaling and Interaction, Cellular Compromise	23
4	Cancer, Hereditary Disorder, Neurological Disease	23
5	Cardiovascular Disease, Cell Morphology, Cellular Growth and Proliferation	2

Figure 4: Functional Analysis (IPA) comparing DMPO vs Ctrl DEGs.

Summary of DEGs in DMPO vs Control comparison was analyzed using Ingenuity Pathway Analysis software in order to identify enriched canonical pathways, networks and upstream signaling.

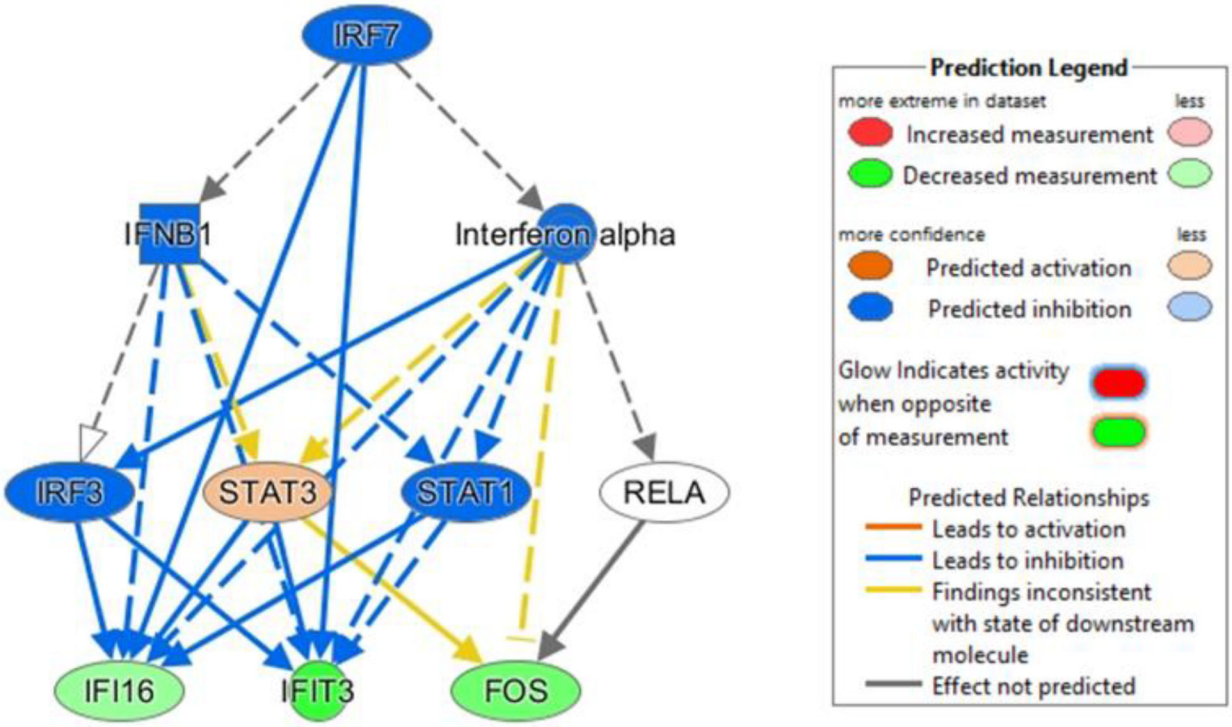

Figure 5: IPA functional analysis for DMPO vs Control DEGs.
Molecules related to IRF7 are predicted as top upstream regulators as displayed.

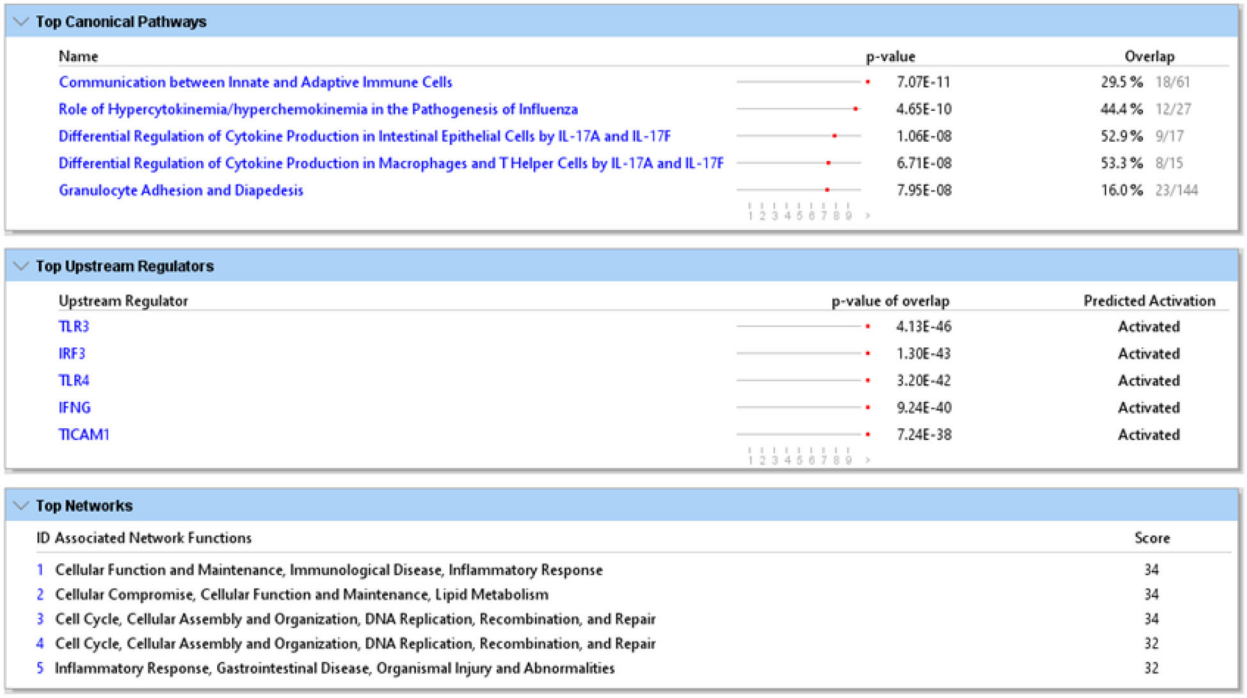

Top Canonical Pathways

Name	p-value	Overlap
Communication between Innate and Adaptive Immune Cells	7.07E-11	29.5 % 18/61
Role of Hypercytokinemia/hyperchemokinemia in the Pathogenesis of Influenza	4.65E-10	44.4 % 12/27
Differential Regulation of Cytokine Production in Intestinal Epithelial Cells by IL-17A and IL-17F	1.06E-08	52.9 % 9/17
Differential Regulation of Cytokine Production in Macrophages and T Helper Cells by IL-17A and IL-17F	6.71E-08	53.3 % 8/15
Granulocyte Adhesion and Diapedesis	7.95E-08	16.0 % 23/144

Top Upstream Regulators

Upstream Regulator	p-value of overlap	Predicted Activation
TLR3	4.13E-46	Activated
IRF3	1.30E-43	Activated
TLR4	3.20E-42	Activated
IFNG	9.24E-40	Activated
TICAM1	7.24E-38	Activated

Top Networks

ID	Associated Network Functions	Score
1	Cellular Function and Maintenance, Immunological Disease, Inflammatory Response	34
2	Cellular Compromise, Cellular Function and Maintenance, Lipid Metabolism	34
3	Cell Cycle, Cellular Assembly and Organization, DNA Replication, Recombination, and Repair	34
4	Cell Cycle, Cellular Assembly and Organization, DNA Replication, Recombination, and Repair	32
5	Inflammatory Response, Gastrointestinal Disease, Organismal Injury and Abnormalities	32

Figure 6: Functional Analysis (IPA) LPS vs Ctrl DEGs:

Analysis summary of DEGs in LPS vs Control comparison using Ingenuity Pathway Analysis software in order to identify enriched canonical pathways, networks and upstream signaling. Analysis summary is shown

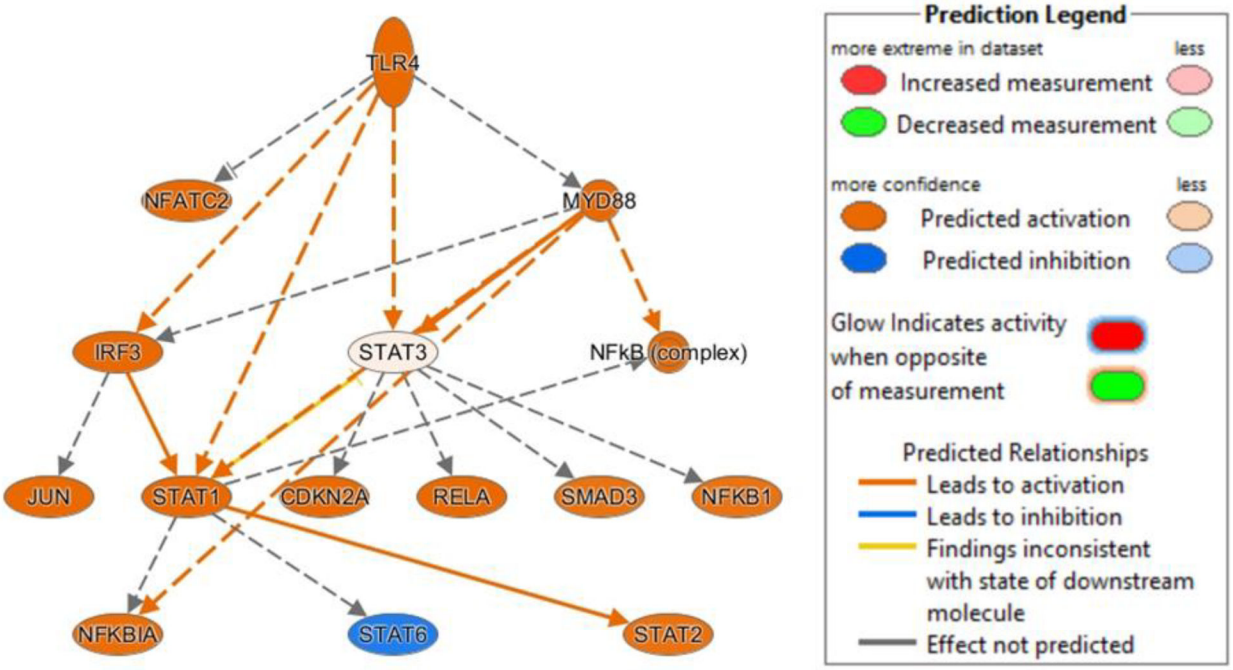

Figure 7: Prediction of TLR4 as upstream regulator.

Molecules related to TLR4 prediction as top 3 upstream regulators are displayed. Fill lines correspond to direct physical interaction. Dashed lines correspond to indirect interaction.

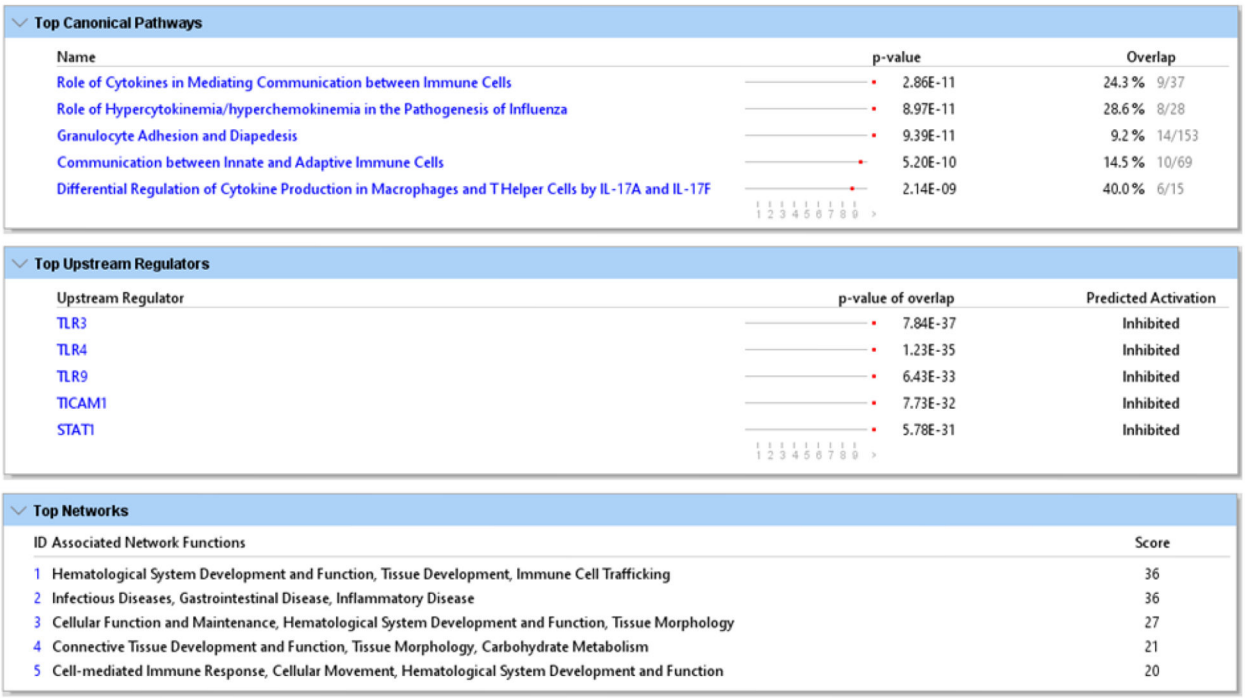

Top Canonical Pathways

Name	p-value	Overlap
Role of Cytokines in Mediating Communication between Immune Cells	2.86E-11	24.3 % 9/37
Role of Hypercytokinemia/hyperchemokinemia in the Pathogenesis of Influenza	8.97E-11	28.6 % 8/28
Granulocyte Adhesion and Diapedesis	9.39E-11	9.2 % 14/153
Communication between Innate and Adaptive Immune Cells	5.20E-10	14.5 % 10/69
Differential Regulation of Cytokine Production in Macrophages and T Helper Cells by IL-17A and IL-17F	2.14E-09	40.0 % 6/15

1 2 3 4 5 6 7 8 9 ›

Top Upstream Regulators

Upstream Regulator	p-value of overlap	Predicted Activation
TLR3	7.84E-37	Inhibited
TLR4	1.23E-35	Inhibited
TLR9	6.43E-33	Inhibited
TICAM1	7.73E-32	Inhibited
STAT1	5.78E-31	Inhibited

1 2 3 4 5 6 7 8 9 ›

Top Networks

ID	Associated Network Functions	Score
1	Hematological System Development and Function, Tissue Development, Immune Cell Trafficking	36
2	Infectious Diseases, Gastrointestinal Disease, Inflammatory Disease	36
3	Cellular Function and Maintenance, Hematological System Development and Function, Tissue Morphology	27
4	Connective Tissue Development and Function, Tissue Morphology, Carbohydrate Metabolism	21
5	Cell-mediated Immune Response, Cellular Movement, Hematological System Development and Function	20

Figure 8: Functional Analysis (IPA) DMPO+LPS vs LPS DEGs: Summary.

DEGs in DMPO+LPS vs LPS comparison were analyzed using Ingenuity Pathway Analysis software in order to identify enriched canonical pathways, networks and upstream. Analysis summary is shown

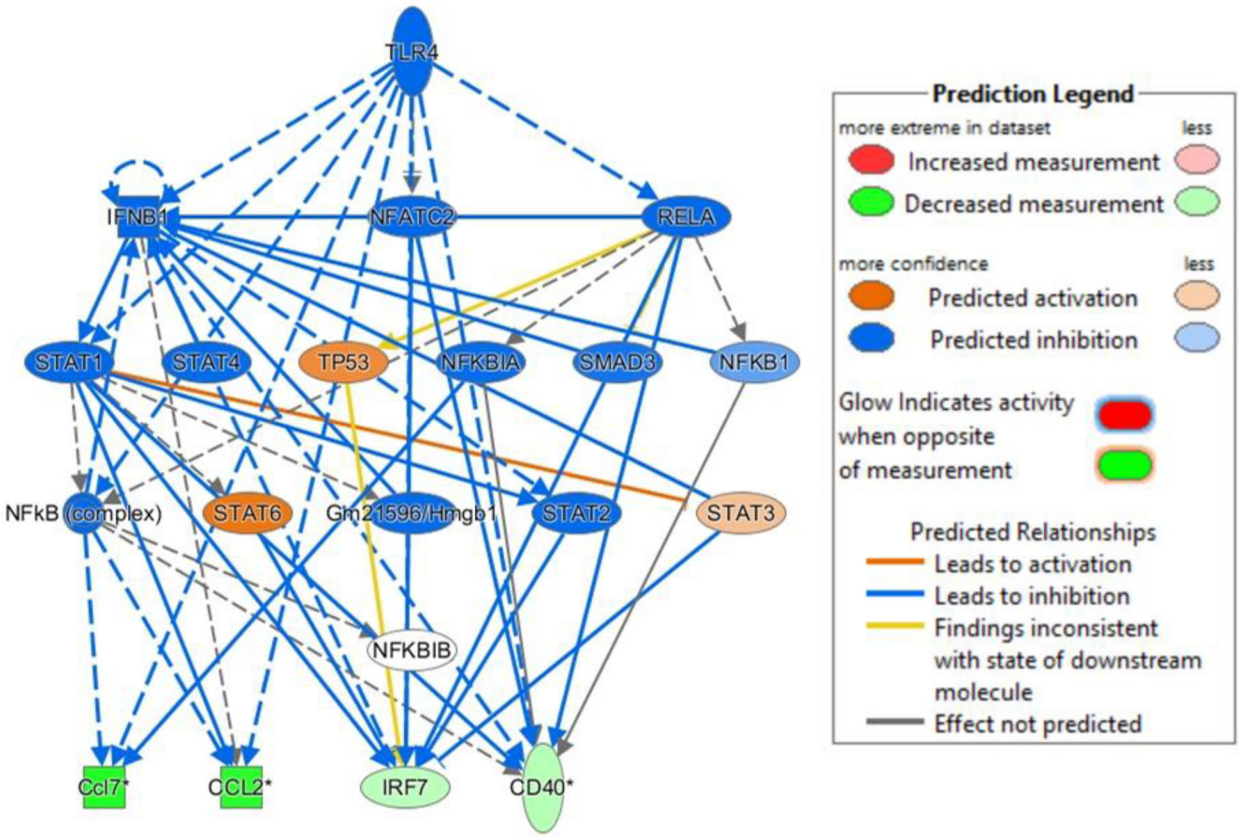

Figure 9: Prediction of TLR4 as upstream regulator.

Molecules related to TLR4 prediction as top 3 upstream regulators are displayed. Fill lines correspond to direct physical interaction. Dashed lines correspond to indirect interaction.

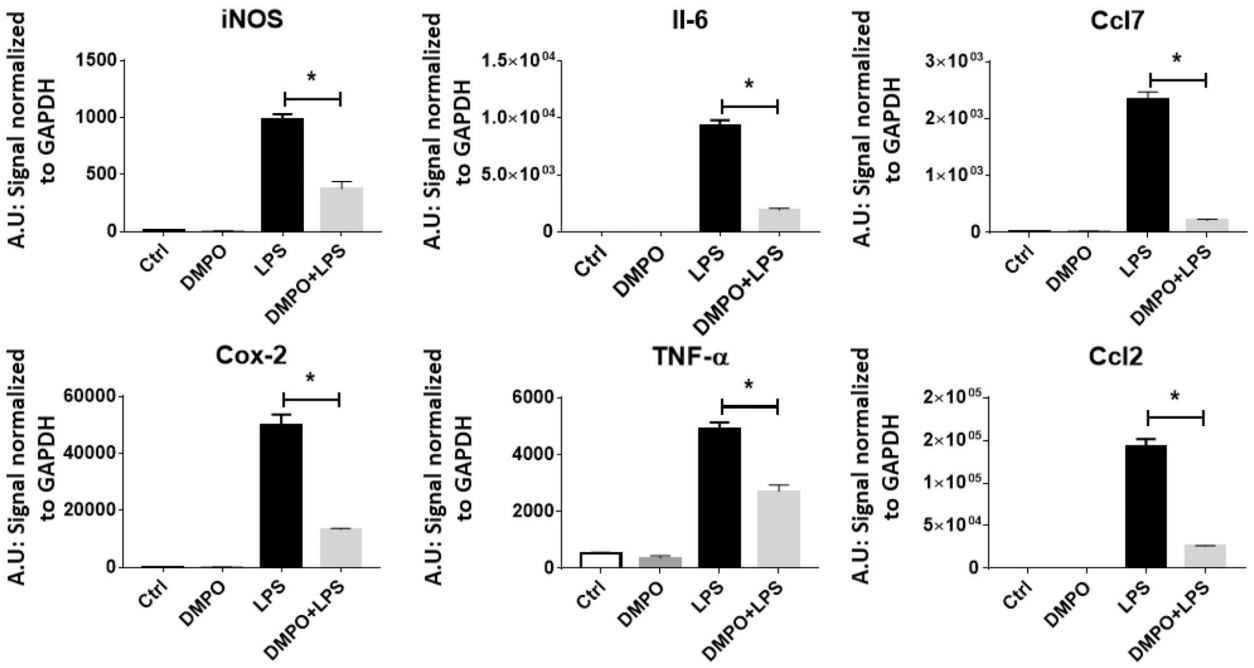

Figure 10: Confirmation of MyD88-dependent pathway inhibition by DMPO in LPS stimulated RAW 264.7 cells.

Cells were treated with 1 ng/ml LPS in the presence or in the absence of 50 mM DMPO for 6 h. After incubation gene expression was examined using the NanoString© platform utilizing Nanostrings Mouse Immunology Codeset (NS_Immunology_C2269). Gene expression was quantified on the nCounter Digital Analyzer™ and raw and normalized counts were generated with nSolver (v3.0)™ software. Genes were normalized to GAPDH signal. One-way ANOVA test was used to determine statistical differences between conditions. *$P < 0.01$.

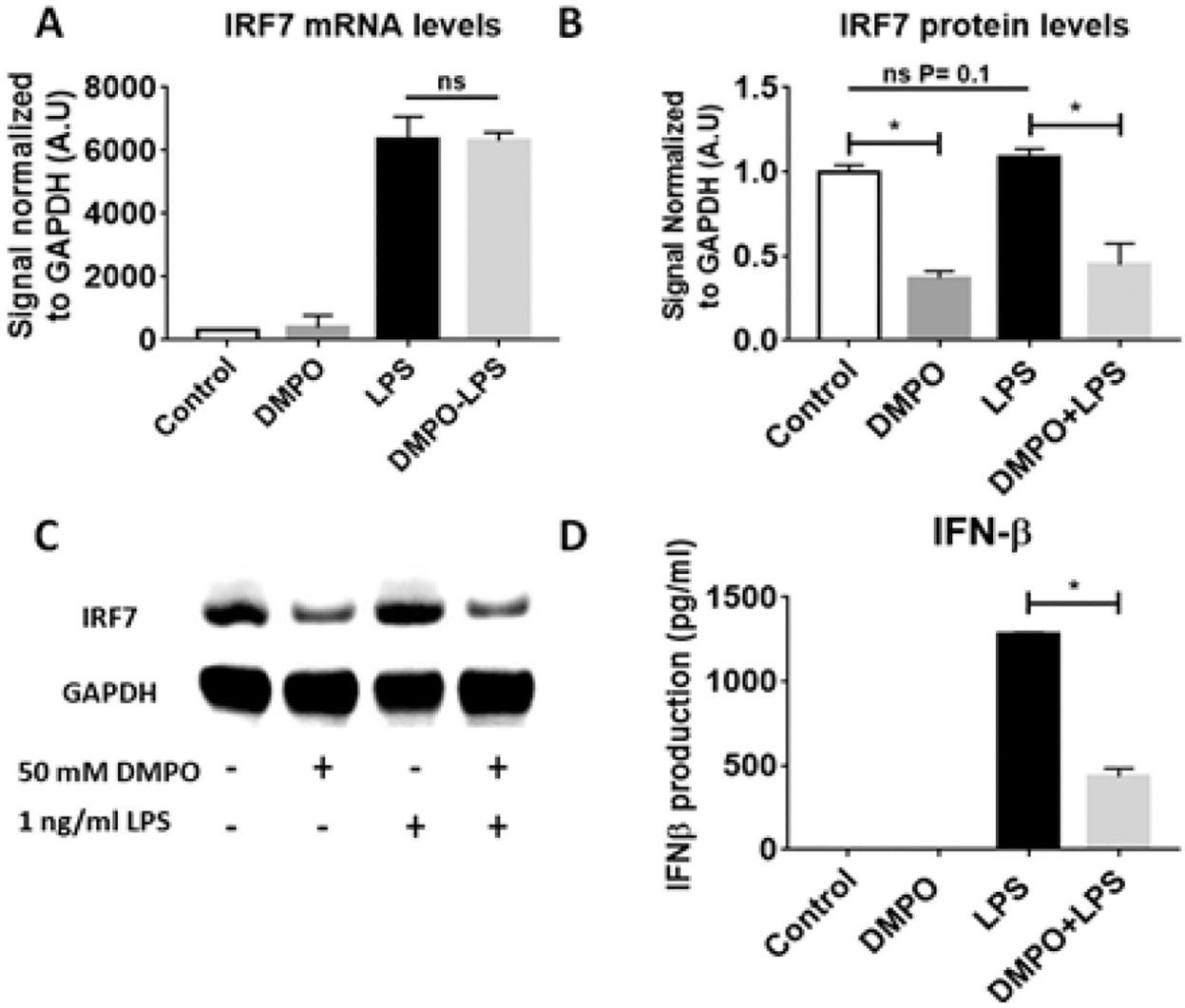

Figure 11: Confirmation of TRIF-dependent pathway inhibition by DMPO in LPS stimulated macrophages.

RAW 264.7 cells were cultured with 1 ng/ml LPS in the presence or absence of 50 mM DMPO for: (A) IRF7 mRNA levels at 6 h after stimulus using nCounter® technology as described in Fig. 10; (B) IRF7 protein determination by western blot at 24 h after stimulus. ImageJ software was used for measuring protein band's optical density. GAPDH was used as loading control. Results are displayed as average of 3 independent experiments; (C) Most representative western blot image of 3 independent experiments were IRF7 protein expression was measured; (D) IFN-β secretion after 24 h stimulus measured by ELISA technique. Results are displayed as average of 3 independent experiments. * $P < 0.01$

Table 1:

DMPO vs Control DEGs: Enriched GO terms

Enriched Gene Ontology (GO) Term	Count	%	PValue	Genes
Response to virus	5	7.69	1.42E-04	IFIT3,0ASL2, EIF2AK2, MX2, DHX58
Transport	16	24.62	3.90E-04	NCBP2, FADS2, STXBP2, SLC7A11, ITPR1, TMEM38B, DAB2, SLC17A6, ARRB2, ATP2A2, TMED3,STXBP5,GLRX…
Endoplasmic reticulum Ca++ homeostasis	3	4.62	8.67E-04	HERPUD1, ATP2A2, ITPR1
Response to endoplasmic reticulum stress	4	6.15	0.002	HERPUD1, ATP2A2, SDF2L1, PDIA6
Defense response to virus	5	7.69	0.002	IFIT3,0ASL2, EIF2AK2, MX2, DHX58
Immune system process	6	9.23	0.007	IFIT3, SMPDL3B, OASL2, EIF2AK2, MX2, DHXS8
Innate immune response	6	9.23	0.008	IFIT3, SMPDL3B, OASL2, EIF2AK2, MX2, DHX58
Response to drug	5	7.69	0.022	LPL, VEGFC, FOS, NPC1, GCLM
Response to toxic substance	3	4.62	0.030	FOS, EIF2AK2, SLC7A11
Negative regulation of cell proliferation	5	7.69	0.033	IFIT3, VEGFC, ASPH, EIF2AK2, TES
Apoptotic process	6	9.23	0.033	DAB2, SGK1, NISCH, CYFIP2, FGF13, ITPR1
Activation of cys-type endopeptidase activity	2	3.08	0.034	CYFIP2, ASPH
Protein transport	6	9.23	0.038	DAB2, ARRB2, TMED3, STXBP5, STXBP2, VPS26B
Negative regulation of toll-like receptor signaling pathway	2	3.08	0.043	ARRB2, SMPDL3B
Negative regulation of innate immune response	2	3.08	0.046	SMPDL3B, DHX58

Table 2:

DMPO vs Control. Top Upstream Regulators

Upstream Regulator	Molecule Type	Predicted	Activation z-score	p-value of overlap	Target molecules in dataset
IRF7	transcription regulator	Inhibited	−2.772	1.86E-10	DHX58,IFI16,IFIT3,ISG15,Mx1/Mx2,Oasl2,PARP12,PHF11
IRF3	transcription regulator	Inhibited	−2.93	4.81E-10	DHX58,EIF2AK2,IFI16,IFIT3,ISG15,Mx1/Mx2,Oasl2,PARP12,PHF11
IFNAR1	transmembrane receptor	Inhibited	−2.219	8.81E-08	E1F2AK2,IFI16,IFIT3,ISG15,Mx1/Mx2,Oasl2,PARP12
IRF5	transcription regulator	Inhibited	−2.219	2.66E-07	DHX58,IFIT3,ISG15,Oasl2,PARP12
TLR3	transmembrane receptor	Inhibited	−2.201	3.98E-07	DHX58,EIF2AK2,FOS,IFI16,IFIT3,ISG15,Mx1/Mx2,Oasl2
TRIM24	transcription regulator	Activated	2.449	7.75E-07	DHX58,IFIT3,ISG15,PARP12,PHF11,UBA7
TLR4	transmembrane receptor	Inhibited	−2.401	6.27E-06	DAB2,IFI16,IFIT3,ISG15,METTL1,Mx1/Mx2,SLC7A11,SMPD13B
NFATC2	transcription regulator	Inhibited	−2	3.21E-05	DAB2,IFIT3,ISG15,ITPR1,Mx1/Mx2
TLR9	transmembrane receptor	Inhibited	−2.415	3.41E-05	IFI16,IFIT3,ISG15,Mx1/Mx2,Oasl2,SMPDL3B
STAT1	transcription regulator	Inhibited	−2.407	8.06E-05	EIF2AK2,IFI16,IFIT3,ISG15,Mx1/Mx2,RNF213

Table 3:

LPS vs Control DEGs: Enriched GO terms

Enriched Gene Ontology (GO) Term	Count	%	PValue	Genes
Inflammatory response	14	20.0	2.81E-10	NFKBIZ, CCL3, CCL2, TNF, LY86, CXCL2, CCL9, CCL4, CCL7, CXCL10, IFI202B, SLC11A1, IL1B, CD14
Chromatin silencing	S	11.4	2.93E-09	HIST1H2AF, HIST1H2AD, HIST2H2AC, HIST1H2AI, H2AFZ, HIST1H2AK, HIST1H2AO, HIST1H2AN
Response to virus	S	11.4	2.26E-08	IFIT3, IFIT2, ODC1, TNF, OASL2, OASL1, EEF1G, CXCL10
Chemokine-mediated signaling pathway	7	10.0	4.72E-08	CCL3, CCL2, CXCL2, CCL9, CCL4, CCL7, CXCL10
Immune response	11	15.7	5.06E-08	CCL3, CCL2, TNF, OASL2, CXCL2, OASL1, CCL9, IL1B, CCL4, CCL7, CXCL10
Neutrophil chemotaxis	7	10.0	1.88E-07	CCL3, CCL2, CXCL2, CCL9, IL1B, CCL4, CCL7
Positive regulation of inflammatory response	6	8.6	3.31E-06	CCL3, CCL2, TNF, CCL9, CCL4, CCL7
Chemotaxis	7	10.0	4.49E-06	CCL3, CCL2, CXCL2, CCL9, CCL4, CCL7, CXCL10
Lipopolysaccharide-mediated signaling pathway	5	7.1	4.73E-06	CCL3, CCL2, TNF, IL1B, CD14
Cellular response to interferon-gamma	6	8.6	4.85E-06	CCL3, CCL2, CCL9, GBP3, CCL4, CCL7
MAPK cascade	6	8.6	5.21E-06	SLC11A1, DOK2, CCL3, CCL2, TNF, IL1B
Lymphocyte chemotaxis	5	7.1	6.12E-06	CCL3, CCL2, CCL9, CCL4, CCL7
Cell chemotaxis	6	8.6	9.54E-06	CCL3, CCL2, CXCL2, CCL9, CCL4, CXCL10
Cellular response to interleukin-1	6	8.6	1.08E-05	CCL3, CCL2, CXCL2, CCL9, CCL4, CCL7
Monocyte chemotaxis	5	7.1	1.34E-05	CCL3, CCL2, CCL9, CCL4, CCL7

Table 4:

DMPO+LPS vs LPS DEGs: Enriched GO terms

Enriched Gene Ontology (GO) Term	Count	%	PValue	Genes
Cellular response to lipopolysaccharide	16	10.4	9.02E-11	CSF3, HAVCR2, CSF2, IL6, CCL2, TNF, IL18, CXCL2, AXL, FCGR4, CD40, CXCL10, LCN2, IRF8, NOS2, GBP2
Inflammatory response	19	12.3	2.00E-10	HAVCR2, NFKBIZ, IL6, CCL2, TNF, PTGS2, NFKBID, IL27, IL18, CXCL2, AXL, CCL9, FPR2, CD40, CCL7, CXCL10, IL1B, FAS, NOS2
Response to virus	10	6.5	1.85E-08	LCN2, IFIT3, IFIT2, TNF, OASL2, OASL1, BCL3, MX2, ISG20, CXCL10
Immune response	15	9.7	2.86E-08	CSF3, CSF2, IL6, CCL2, TNF, IL18, CXCL2, CCL9, CCL7, CXCL10, OASL2, IRF8, OASL1, IL1B, FAS
Immune system process	17	11.0	5.21E-08	HAVCR2, CFB, IL27, AXL, PTPN22, SAMHD1, CD40, FCGR1, ISG20, IFIT3, LCN2, IFIT2, OASL2, IRF7,TAP1, OASL1, MX2
Defense response to virus	11	7.1	7.52E-07	IFIT3, IFIT2, IL6, IFNB1, OASL2, OASL1, SAMHD1, CD40, MX2, ISG20, CXCL10
Cellular response to interferon-gamma	8	5.2	9.84E-07	CCL2, EDN1, CCL9, SYNCRIP, NOS2, GBP3, GBP2, CCL7
Innate immune response	15	9.7	3.03E-06	HAVCR2, CFB, IL27, AXL, SAMHD1, FCGR1, ISG20, IFIT3, LCN2, IFIT2, IFNB1, OASL2, IRF7, OASL1, MX2
Defense response to protozoan	6	3.9	3.27E-06	IL6, IRF8, BCL3, CD40, GBP3, GBP2
Response to lipopolysaccharide	11	7.1	3.36E-06	TNF, PTGS2, CXCL2, EDN1, IL1B, PTPN22, NOS2, FAS, CD40, GCH1, CXCL10
Chromatin silencing	7	4.5	9.53E-06	HIST1H2AF, HIST1H2AD, HIST2H2AC, HIST1H2AI, HIST1H2AH, HIST1H2AK, HIST1H2AN
Cellular response to interferon-beta	6	3.9	1.61E-05	IFIT3, IFNB1, IFI47, GBP3, GBP2, IFI205
Response to glucocorticoid	7	4.5	2.62E-05	IL6, TNF, PTGS2, ASS1, IL1RN, CXCL2, FAS
Positive regulation of smooth muscle cell proliferation	7	4.5	3.78E-05	EGR1, IL6, TNF, PTGS2, IL18, EDN1, CALCRL
Cellular response to interleukin-1	7	4.5	3.78E-05	LCN2, IL6, CCL2, CXCL2, EDN1, CCL9, CCL7

Table 5:

DMPO+LPS vs LPS DEGs: Enriched KEGG pathways

Enriched KEGG Pathway	Count	%	PValue	Genes
TNF signaling pathway	13	8.4	4.96E-10	CSF2, IL6, CCL2, TNF, PTGS2, MMP9, EDN1, CXCL2, IFI47, CXCL10, BCL3, IL1B, FAS
Cytokine-cytokine receptor interaction	13	8.4	4.08E-06	CSF3, VEGFC, CSF2, IL6, TNF, CCL2, IFNB1, IL18, IL1B, FAS, CD40, CCL7, CXCL10
Hematopoietic cell lineage	8	5.2	1.67E-05	CSF3, CSF2, IL6, TNF, CD44, CD33, IL1B, FCGR1
Cytosolic DNA-sensing pathway	6	3.9	3.93E-04	IL6, IFNB1, IRF7, IL18, IL1B, CXCL10
Toll-like receptor signaling pathway	7	4.5	4.51E-04	IL6, TNF, IFNB1, IRF7, IL1B, CD40, CXCL10
Transcriptional misregulation in cancer	8	5.2	0.00117749	CSF2, NFKBIZ, IL6, CDKN2C, MMP9, CD40, FCGR1, DDIT3
Natural killer cell mediated cytotoxicity	5	3.2	0.01962618	CSF2, TNF, IFNB1, FCGR4, FAS
RIG-I-like receptor signaling pathway	4	2.6	0.02910377	TNF, IFNB1, IRF7, CXCL10
Osteoclast differentiation	5	3.2	0.03526152	TNF, IFNB1, FCGR4, IL1B, FCGR1
MAPK signaling pathway	7	4.5	0.03785582	TNF, MKNK2, IL1B, FAS, DAXX, DDIT3, DUSP6

Table 6:

DMPO+LPS vs LPS. Top Upstream Regulators

Upstream Regulator	Molecule Type	Predicted Activation State	Activation z-score	p-value of overlap	Target molecules in dataset
TLR3	transmembrane receptor	Inhibited	−5.577	7.84E-37	BCAR3,Ccl2,Ccl7,CD40,CD69,CSF2,CSF3,CXCL10,CXCL3,EDNl,FAS,GBP2,GBP3,GBP4,GCH1,
TLR4	transmembrane receptor	Inhibited	−5.296	1.23E-35	Ccl2,CCL2,Ccl7,CD40,CFB,CSF2,CSF3,CXCL10,CXCL3,DAB2,DAXX,EDNl,FAS,GBP2,HDC,IFI
TLR9	transmembrane receptor	Inhibited	−5.415	6.43E 33	Ccl2,Ccl7,CD40,CD69,CSF2,CSF3,CXCL10,CXCL3,EDNl,EGRl,FAS,GCH1,IFI16,IFIT2,IFIT3,IFN
TICAM1	other	Inhibited	−4.782	7.73E-32	BCL3,Ccl2,CCL2,CD40,CFB,CXCL10,CXCL3,EGRl,ETS2,FAS,FPR2,IFIl6,Ifi47,IFIT2,IFIT3,IFNE
STAT1	transcription regulator	Inhibited	−5.025	5.78E-31	AXL,Ccl2,CCL2,CD40,CSF2,CXCL10,CXCL3,EGRl,FAS,GBP2,GBP3,IFI16,Ifi47,IFIT2,IFIT3,IFN
IRF3	transcription regulator	Inhibited	−3.506	1.60E-28	Ccl2,CD40,CD69,CXCL10,DAXX,FAS,FCGRlA,IFI16,Ifi47,IFIT2,IFIT3,IFNBl,ILlB,IL27,IL6,IRF7
IFNAR1	transmembrane receptor	Inhibited	−2.458	5.68E-28	Apol9a/Apol9b,AXL,Ccl9,CD40,CXCL10,CXCL3,DUSP6,IFI16,IFIT2,IFIT3,IFNBl,IL18,ILlB,IL27
MYD88	other	Inhibited	−5.028	1.44E 27	BCL3,Ccl2,CD40,CD44,CSF2,CSF3,CXCL10,CXCL3,DAXX,EGRl,ETS2,FPR2,HDC,IFIT2,IFNB1
PTGER4	g-protein coupled receptor	Activated	4.61	2.00E-27	Ccl2,CCL2,Ccl7,CD40,CD69,CXCL10,DAXX,EDNl,GBP2,GBP4,HAVCR2,HERPUDl,IFI16,Ifi47,I
IFNG	cytokine	Inhibited	−5.66	1.46E-26	BCL3,Ccl2,CCL2,Ccl7,CD40,CD44,CSF2,CSF3,CXCL10,CXCL3,DDIT3,EDNl,FAS,GBP2¡GBP3,C